

# LBV Nebulae: The Mass Lost from the Most Massive Stars

Kerstin Weis

Institut für Theoretische Astrophysik

Universität Heidelberg

Tiergartenstr. 15

69121 Heidelberg

kweis@ita.uni-heidelberg.de

<http://www.ita.uni-heidelberg.de/~kweis>

## Abstract

*The most massive stars, with initial masses above  $\sim 50 M_{\odot}$ , encounter a phase of extreme mass loss—sometimes accompanied by so-called giant eruptions—in which the stars' evolution is reversed from a redward to a blueward motion in the HRD. In this phase the stars are known as Luminous Blue Variables (LBVs). Neither the reason for the onset of the strong mass loss nor the cause for the giant eruptions is really understood, nor is their implications for the evolution of these most massive stars. I will present a study of the LBV nebulae which are formed in this phase as a consequence of the strong mass loss and draw conclusions from the morphology and kinematics of these nebulae on possible eruption mechanisms and stellar parameters of the LBV stars. The analysis contains a large collection of LBV nebulae which form an evolutionary sequence of LBV nebulae. A special concern will be the frequently observed bipolar nature of the LBV nebulae which seems to be a general feature and presents strong constraints on further models of the LBV phase and especially on the formation mechanism of the nebulae.*

## 1 Introduction

Due to their brightness, massive stars can be investigated as individual objects even in neighboring galaxies. They have initial masses between  $\sim 15 M_{\odot}$  and  $120 M_{\odot}$ , bolometric luminosities of  $10^5$  to  $10^6 L_{\odot}$  and they live about  $2 - 10 \cdot 10^6$  years (eg., Schaller et al. 1992, Maeder & Conti 1994, Schaerer et al. 1996a, 1996b). Through stellar winds these stars loose a sizeable fraction of their initial mass during their life (already more than 50% during the main-sequence phase) corresponding to an average mass loss rate of  $10^{-5} \dots 10^{-6} M_{\odot} \text{yr}^{-1}$  (eg., de Jager et al. 1988, Kudritzki et al. 1996, Kudritzki 1999) which compares to the loss of low mass stars like the Sun of  $\sim 10^{-14} M_{\odot} \text{yr}^{-1}$ . Only in recent years it has become obvious that this mass loss strongly influences

the stellar evolution (eg., Chiosi & Maeder 1986) and both, directly and due to the change in evolution, has strong implications on the evolution of the interstellar and circumstellar environment. Massive stars therefore not only are major contributors of high energy photons which excite for example H II regions, they also—through their winds—supply a large amount of kinetic energy into the surrounding medium. Their largest input, however, is still given as these stars explode as supernovae at the end of their evolution.

Stars with masses above  $M \sim 50 M_{\odot}$  and luminosities of  $L \sim 10^6 L_{\odot}$  top the *Hertzsprung-Russell Diagram* (HRD) and represent the most massive stars known. After spending a ‘normal’ life as O stars on the main sequence, they evolve towards cooler temperatures and enter a phase with—even for their standards—*extremely* high mass loss (up to  $10^{-3...-4} M_{\odot} \text{yr}^{-1}$ ) and become *Luminous Blue Variables* (LBVs; Langer et al. 1994, Humphreys & Davidson 1994, Maeder & Meynet 2000). In the HRD, the LBV phase starts when the stars reach the empirical *Humphreys-Davidson limit* (Humphreys & Davidson 1979, Humphreys & Davidson 1994). It seems as if the most massive stars do not evolve beyond this limit towards lower temperatures. They rather turn around, evolve back and become blue supergiants located in the HRD in the vicinity of the Humphreys-Davidson limit. Moreover, this is the location in the HRD where those stars undergo extremely strong mass loss through winds and occasional giant eruptions (eg., Humphreys 1999), and thus peel off parts of the stellar envelope. The LBV stars therefore often form small circumstellar nebulae, the *LBV nebulae* (eg., Nota et al. 1995). For a compilation of LBV nebulae known today, see Table 1. The formation of the nebulae as well as the consequences of the mass loss on the evolution of the most massive stars, especially in the LBV phase, is still far from being understood. In particular it is neither clear what causes the strong mass loss to set in, and thus to reverse the direction of the star’s evolution in the HRD, nor what leads to the giant eruptions. Their closeness to the classical Eddington limit, however, makes a loss of radial balance not very surprising.

First hydrodynamic calculations modeled the formation of LBV nebulae through the interaction of slow and fast winds in the stars’ evolution. The model by García-Segura et al. (1996), for instance, was calculated for a  $60 M_{\odot}$  star, and shows that the slow wind in the beginning of the LBV phase is swept up by the following faster wind and compressed into a thin shell, which manifests itself as an LBV nebula. This wind-wind interaction model predicts an expansion velocity of about  $\sim 240 \text{ km s}^{-1}$  for the nebula and that, due to the mixing up and peeling off of material from the CNO cycle, the nitrogen abundance is enhanced by a factor of about  $\sim 13$ . While this model may be able to explain the formation of LBV nebulae formed by stellar wind, LBV nebulae which were created in a giant eruption these models are not able to account for. In giant eruptions the LBVs increase their brightness by typically 2 – 5 magnitudes within only a few years (see for example Fig. 1(b) in Humphreys et al. 1999 for P Cygni). The total energy output during such an event is  $\sim 10^{50}$  ergs and therefore nearly comparable to a supernova—actually there were two giant eruption LBVs which were originally mistaken

Table 1: Parameters of known LBV nebulae

LBV	host galaxy	size [pc]	$v_{\text{exp}}$ [km s <sup>-1</sup> ]	references
$\eta$ Carinae	Milkyway	0.2/0.67	600/10 – 2000	1, 2
HR Carinae	Milkyway	$1.3 \times 0.65$	75 – 150	3, 4
P Cygni	Milkyway	0.2/0.8	110 – 140/185	5
AG Carinae	Milkyway	$0.87 \times 1.16$	70	6
WRA 751	Milkyway	0.5	26	7
He 3-519	Milkyway	2.1	61	8
HD 168625	Milkyway	$0.13 \times 0.17$	40	9
Pistol Star	Milkyway	$0.8 \times 1.2$	60	10
R127	LMC	1.3	32	11
R143	LMC	1.2	24 (?)	11
S61	LMC	0.82	27	11
S119	LMC (?)	1.8	26	12
Sher 25	Milkyway	1	70	13, 14
Sk-69° 279	LMC	4.5	14	15, 16

(1) Davidson & Humphreys (1997), (2) this work, (3) Weis et al. (1997a), (4) Nota et al. (1997), (5) Meaburn et al. (1996a), (6) Nota et al. (1992), (7) Weis (2000a), (8) Smith et al. (1994), (9) Nota et al. (1996), (10) Figer et al. (1999), (11) Weis (2000b), (12) Weis et al. (2000a), (13) Brandner (1997a), (14) Brandner (1997b), (15) Weis et al. (1997b), (16) Weis & Duschl (2000).

for supernova explosions (Humphreys 1999), namely SN 1961V (in NGC 1058) and SN 1954J (in NGC 2403). Simple wind-wind interaction models are not able to get such outbursts and the formation of the LBV nebula on such short timescales. The outburst phases are not longer than a few years, while the formation of a nebula due to interaction of winds takes at least several  $10^3$  years, according to the model of García-Segura et al. (1996).

As yet, only a few LBVs are known in our Galaxy (8 objects plus candidates) and some more in other galaxies, like the Large Magellanic Cloud (LMC), M31 and M33 (Humphreys & Davidson 1994). Altogether around 40 LBV stars are currently known, many of which show circumstellar nebulae. To better understand the LBV phase and especially the formation of the LBV nebulae, and the onset of the enhanced mass loss, in order to address the question what causes the evolution of the most massive stars to reverse, I have analyzed the nebulae of most of the LBVs known. What increases the mass loss in the LBV phase? What drives the giant eruptions, what mechanism forms instabilities that might lead to the eruptions? And, how do the nebulae form? Only if we can answers these questions we well be able to better understand the structure and evolution of the most massive stars.

## 2 The Nebula around the LBV $\eta$ Carinae

### 2.1 Historical Background

$\eta$  Carinae, perhaps the best-known of all LBVs, is located in NGC 3372, one of the largest H II regions in our Galaxy. It is often referred to as the *Carina Nebula*.  $\eta$  Carinae belongs to the Trumpler 16 cluster (Massey & Johnson 1993, Walborn 1995) which is close to the central region of NGC 3372 which, in turn is known as the *Keyhole nebula* (see Fig. 1), at a distance of about 2.3 kpc from us (Walborn 1995).  $\eta$  Carinae has a bolometric luminosity of  $L = 10^{6.7} L_{\odot}$  which puts the star among the most luminous stellar objects and—with an estimated mass of about  $120 M_{\odot}$ —also among the most massive stars in our Galaxy (Humphreys & Davidson 1994, Davidson & Humphreys 1997). Even if recent indications of a binary nature of  $\eta$  Car (see Damineli 1996, Damineli et al. 1997, Stahl & Damineli 1998) prove to be true, at least one component must be within the range of LBVs, i.e., larger than  $\sim 50 M_{\odot}$ . The binary hypothesis is highly under debate still. Since it is not a crucial constraint for the work presented here this issue will not be addressed further. For detailed discussions, we refer the reader to the above mentioned references.

Historical observations of  $\eta$  Carinae showed that the star is variable and changed between 4<sup>m</sup> and 2<sup>m</sup> in the 17th and 18th century. The star’s most peculiar behavior, however, was its outburst around 1843 when it increased its visual magnitude to  $-1^m$  for a short time ( $\sim 10$  years) before its luminosity declined by 7 magnitudes in only a few years— $\eta$  Carinae had undergone a giant eruption. For lightcurves, see, for example, Gratton (1963), Viotti (1995), and Humphreys (1999).

During this eruption a circumstellar LBV nebula had formed which was not detected until 1938 when van den Bos noted a *nebula halo* when observing components of  $\eta$  Carinae which he thought were parts of a multiple system. Only around 1950 it became clear that these components were brighter knots of a fainter nebula. Nearly simultaneously but independently Gaviola (1946, 1950) and Thackeray (1949, 1950) discovered and photographed this nebula for the first time. Due to the odd man-like shape of the nebula Gaviola named it the *Homunculus*. Gaviola also noted that there may be a much fainter and larger hook-shaped nebula surrounding the Homunculus. Indeed there was an outer nebula. Deeper images by Walborn (1976) showed such a larger nebula which consists of structures as, for instance, the *S ridge*, the *E condensations*, or the *W arc* (for a complete description see the sketch by Walborn 1976). It was not until 1995 that the first high-resolution images were published: a ground based image (Duschl et al. 1995), which was already taken in 1985 and re-constructed by a *shift-and-add-like* technique, and the first (COSTAR corrected) HST images taken in 1993 (eg., Morse et al. 1998). The images reveal that the morphology of the Homunculus nebula is highly bipolar. Two lobes are separated by an equatorial disk (Duschl et al. 1995) which is defined by structures called streamers. The HST image in Fig. 1 shows very well the bipolar nebula and the equatorial disk. A careful inspection of the images

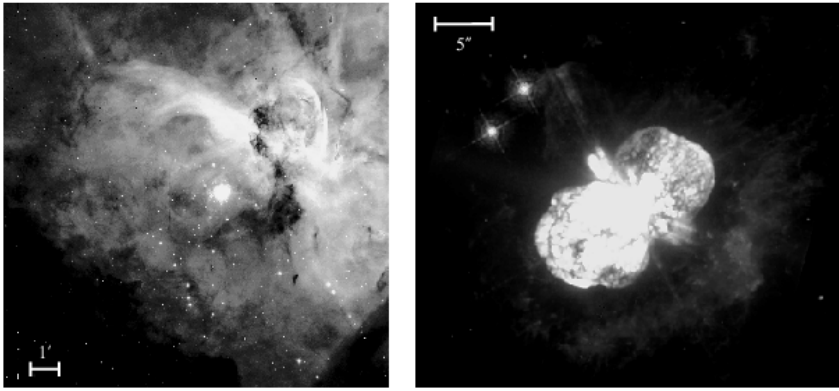


Figure 1: *Left:* This figure shows an  $H_\alpha$  image, taken with the CTIO 0.9 m telescope of the central region in NGC 3372, called the Keyhole nebula. The keyhole shaped nebula is visible as well as a bright, extended source to the east which is the LBV  $\eta$  Carinae and its nebula. The field of view is about  $13' \times 13'$ , east is left and north to the top. *Right:* An HST image reveals clearly the bipolar nature of the Homunculus nebula around  $\eta$  Carinae. Again east is left and north to the top.

reveals that the Homunculus shaped nebula, reported earlier, manifests only the brightest structures within the bipolar nebula. An even longer exposure (200 s) with the HST (see Fig. 2) in the F656N ( $H_\alpha$ ) filter detects a large amount of filaments and knots in addition to the structures already known outside of the Homunculus (as reported by Walborn 1976).

First measurements of the expansion of the Homunculus nebula were published by Ringulet (1958) and Gratton (1963). They reach to values of  $500 \text{ km s}^{-1}$  for the expansion (corrected to today's distance determination of  $\eta$  Car). A very detailed analysis of proper motion measurements, again for some of the outer filaments, has been made in a series of studies by Walborn (1976), Walborn et al. (1978) and Walborn & Blanco (1988), in which they find tangential velocities between  $280 \text{ km s}^{-1}$  and  $1360 \text{ km s}^{-1}$ . Recent proper motion measurement using the high-resolution HST images support these results: Currie et al. (1996) and Currie & Dowling (1999) obtain values between 10 and  $1000 \text{ km s}^{-1}$  as do Smith & Gehrz (1998) through a comparison of old ground based images with a resolution-degraded HST image, enlarging the time base. Thackeray (1961) was among the first to derive radial velocities from spectra. Comparing forbidden and permitted lines he concluded that the Homunculus expands with  $630 \text{ km s}^{-1}$ . Later studies using a long-slit mode show even higher values for structures outside the Homunculus. Meaburn et al. (1987, 1993a, 1993b, 1996b) report on radial velocities from at least  $250 \text{ km s}^{-1}$  to  $-1200 \text{ km s}^{-1}$ , with an additional uncertain feature at  $-1450 \text{ km s}^{-1}$ . Fabry-Perot measurements (Walborn 1991) agree with these values.

## 2.2 Morphology

In order to analyze the morphology of the nebula around  $\eta$  Carinae we used deep high-resolution images from the HST archive. Figure 2 shows a F656N filter image. Note that this image is showing not only  $H_\alpha$  emission but in addition red- and blueshifted emission from the  $[\text{N II}]$  lines at  $6548 \text{ \AA}$  and  $6583 \text{ \AA}$ . Due to the large Doppler shift (above  $1000 \text{ km s}^{-1}$ ) of at least some of the filaments, parts of the nebula's emission in the F656N filter is ambiguous. The brightness levels displayed in this image are optimized to especially reveal faint structures in the outskirts of the nebula. The bipolar Homunculus is unresolved as the oval shaped saturated central part. While the Homunculus measures about  $17''$  (about  $0.2 \text{ pc}$ ) across, fainter structures are detected up to distances of  $30''$  ( $0.33 \text{ pc}$ ) from the star. All knots outside the Homunculus taken together form the *outer ejecta*. Knots and condensations classified earlier by Walborn (1976) are part of these outer ejecta.

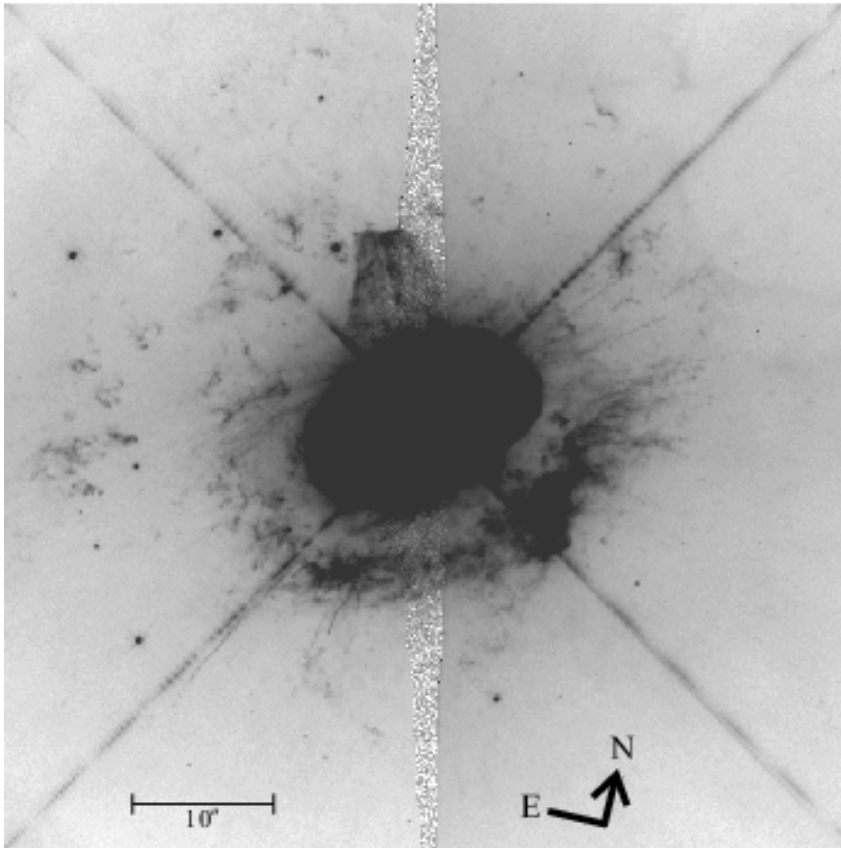


Figure 2: This figure shows an HST image taken with the F656N filter ( $H_\alpha$ ) of the nebula around the LBV  $\eta$  Carinae. The field of view is about  $60'' \times 60''$ .

The knots and filaments in the outer ejecta consist of very different morphological shapes and sizes. They can be described as bullets, long filaments, some even look like arches—but one has to keep in mind that all structures are only seen in projection. The sizes of coherent structures vary from as large as  $7''.5$  ( $0.08$  pc, the *N Condensation*) down to fractions of arcseconds (several  $10^{-3}$  pc)—the limit of what HST can resolve. Most likely the outer ejecta contains numerous even smaller and/or fainter structures below the detection limit of this image. One of the most striking features are very straight, long and collimated objects which in the following we will call *strings*. These structures will be discussed in Section 2.4.

An area in the outer ejecta particularly rich in structures like bullets and filaments is the *S ridge* (with the brightest part called the *S Condensation*, Walborn 1976). The deep HST image (Fig. 2) shows in great detail the countless knots present in a nearly circular ring around  $\eta$  Carinae with long filaments pointing roughly radially outwards in this ridge. An analysis of the X-ray emission from the nebula around  $\eta$  Carinae (Weis et al. 2000b) supports that most likely high-velocity knots colliding with their environment are present in the *S ridge* and give rise at this position to the highest X-ray emission from the nebula.

### 2.3 Kinematics and 3D Structure

For a detailed study of the kinematics of the nebula—which will help to better model and understand its 3 dimensional structure—high-resolution echelle long-slit observations were made, using the Cerro Tololo Inter-American Observatory’s 4 m telescope. The instrumental FWHM of the spectra at the  $H_\alpha$  line was about  $14 \text{ km s}^{-1}$ . With spacings of the offsets chosen to match the seeing ( $1''.5$ ) a complete 2 dimensional mapping was secured, taking 31 spectra and covering an area of about  $1' \times 1'$  ( $0.67 \text{ pc} \times 0.67 \text{ pc}$ ). A position angle (PA) of  $132^\circ$  was chosen, putting the slits parallel to the major axis of the Homunculus. Due to strong stray-light from the central star the central 6 slit positions could not be used.

Figure 3 depicts 3 echellograms taken at different positions. The spatial axis in each echellogram is  $90''$  high, the spectral axis covers  $75 \text{ \AA}$  centered on  $H_\alpha$  at its rest wavelength. Beside the splitted line emission (split by about  $40 \text{ km s}^{-1}$ ) across the entire spectrum, which results from the background H II region, a large variety of blue- and redshifted knots from the nebula around  $\eta$  Carinae is visible in the spectra (Fig. 3).

The maximum and minimum velocities of each knot identified in the spectra were measured, together with the velocities of the brightest intensity maxima of a knot. The knots as identified from the spectra were compared with and re-identified in the HST images. More than 200 individual knots in the spectra were found and, as seen in Fig. 3, nearly all of them show substructures. A knot is defined as a single entity if it shows a coherent appearance in the spectra. For example knot 1 in Slit 10S is a single feature as is knot 7 in Slit 10S. Substructure means that these structures are coherent but show different

intensities or a change in the velocity profile (e.g. knot 7 in Slit 10S). Taking all spectra together we obtain the following overall properties: The fastest blueshifted structure moves with a maximum radial velocity of  $-1200 \text{ km s}^{-1}$ , the fastest redshifted features reach up to  $+2000 \text{ km s}^{-1}$ . The majority of the knots shows radial velocities reaching between  $-600 \text{ km s}^{-1}$  and  $+600 \text{ km s}^{-1}$  (would these structures have a projection angle of  $45^\circ$  the unprojected velocities were already between  $-850 \text{ km s}^{-1}$  and  $+850 \text{ km s}^{-1}$ ). The largest velocity spread of one single coherent structure is as high as  $1250 \text{ km s}^{-1}$ .

The spectra also allow us to obtain the line ratio  $[\text{N II}]\lambda 6583\text{\AA}/\text{H}\alpha$  leaving a hint for the strength of nitrogen within the nebula. As stated above an enhanced nitrogen ratio is expected due to the overabundance of nitrogen in the nebula which results from the CNO cycled material peeled off from the star. For the structures measured in the outer ejecta this  $[\text{N II}]\lambda 6583\text{\AA}/\text{H}\alpha$  ratio shows values between 1 – 5 with a peak around 3.

Beside the kinematic information for each individual structure the measurements show an interesting global result. An overlay of respective knots onto an HST image as given in Fig. 4 clearly shows the trend that blueshifted structures appear in the south-east while redshifted are concentrated to the north-west. The knots in the outer ejecta—which seem to be randomly distributed around  $\eta$  Carinae—seem to follow an ordered kinematic pattern. They are moving in a bipolar mode with respect to the central star. Knots in the south-east are approaching us, while knots north-west of  $\eta$  Carinae move away from the observer. Going even further and comparing the bipolar structure of the outer ejecta with the inner central bipolar Homunculus we can see that both parts of the nebula follow the same symmetry. The south-eastern lobe of the Homunculus is tilted towards the observer (the net expansion here is therefore blueshifted—approaching) while the north-western lobe is tilted to the back (redshifted—receding). This bipolarity is repeated in the filamentary outer ejecta with the same symmetry and with about the same symmetry axis, i.e., both the Homunculus and the outer ejecta exhibit a very similar bipolar structure of the nebula around  $\eta$  Carinae.

## 2.4 Strings—a new Phenomena in LBV Nebulae?

Among the structures detected within the outer ejecta are the so-called *strings*. They are very straight, highly collimated structures which reach lengths comparable to the diameter of the entire Homunculus. For a detailed analysis of these objects the reader is referred to Weis et al. (1999). In the nebula around  $\eta$  Carinae 5 strings have been identified by visual inspection of the HST images (Fig. 5). On much smaller scales a large number of string-like objects can be found in the outer ejecta. We do not count these smaller structures as strings since their collimation and parameters are not as extreme as for the strings.

The longest one is string1 with an observed length of  $15''.9$  or  $0.18 \text{ pc}$ . At the same time string1 is only  $0''.23$  wide ( $0.003 \text{ pc}$ ) which corresponds to a length-to-width ratio of 70, underlining the strong collimation of these objects.

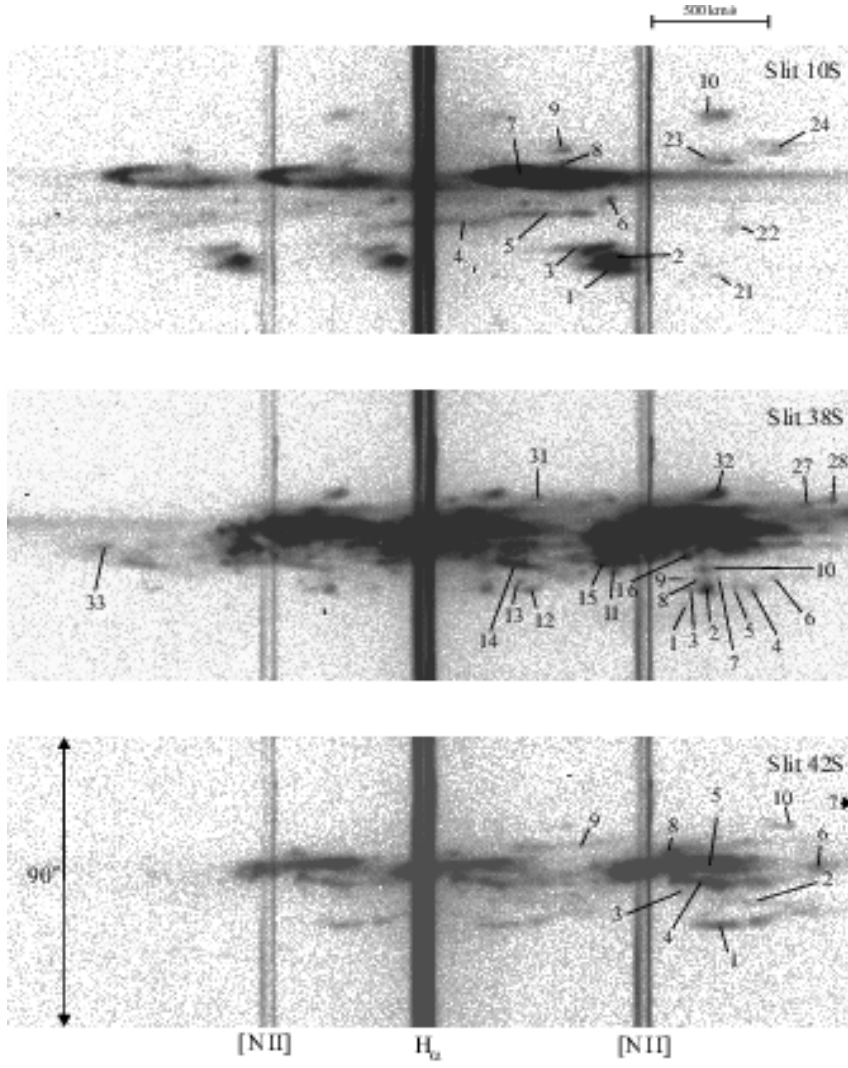


Figure 3: The echellograms displayed here are 90'' high in spatial direction and cover a spectral region of 75 Å centered on rest-wavelength H $\alpha$ . In many cases redshifted as well as blueshifted knots appear simultaneously, producing the ‘messy spectra’. Since all knots are present in all 3 lines included in the spectra an unambiguous identification was nevertheless possible for most of them.

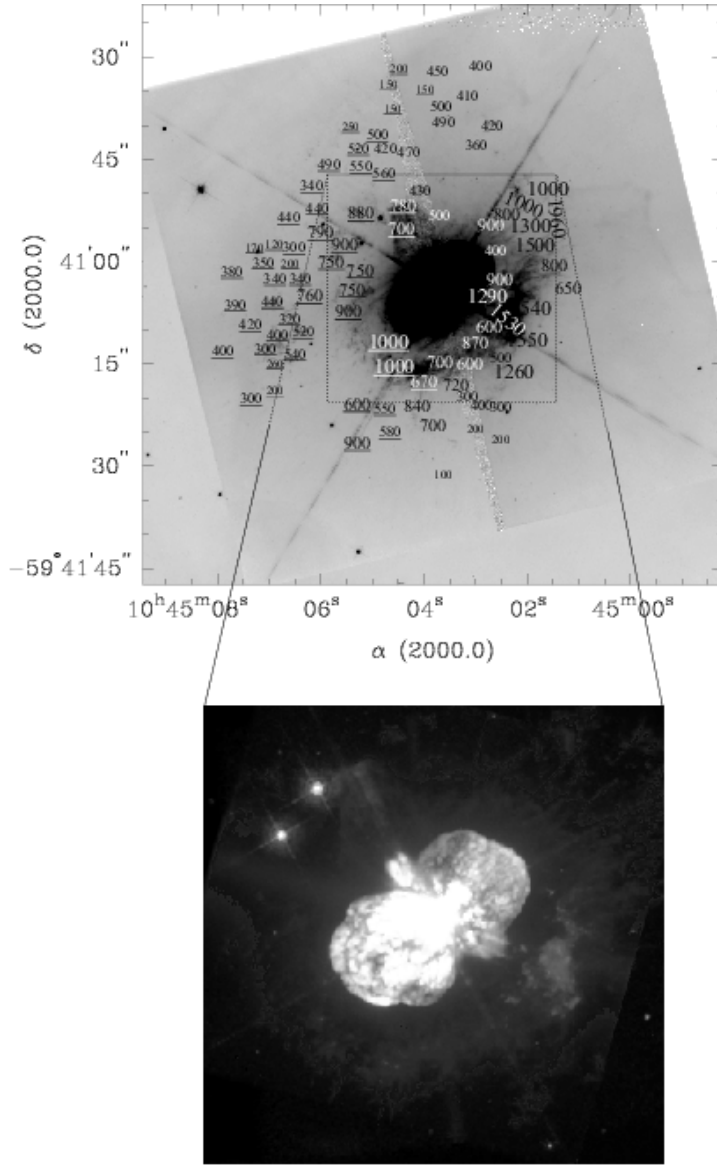


Figure 4: In the upper panel the same image as in Fig. 2 is shown. Onto the image, scaled by font sizes, the radial velocities of individual knots (with the highest velocity for a certain area) are overplotted. Underlined velocities represent negative (blueshifted) structures, not underlined are redshifted, positive values. A clear trend is visible: blueshifted structures appear preferentially in the south-east while redshifted are concentrated to the north-west. The lower panel shows the central bipolar Homunculus for comparison. In both images north is up and east to the left.

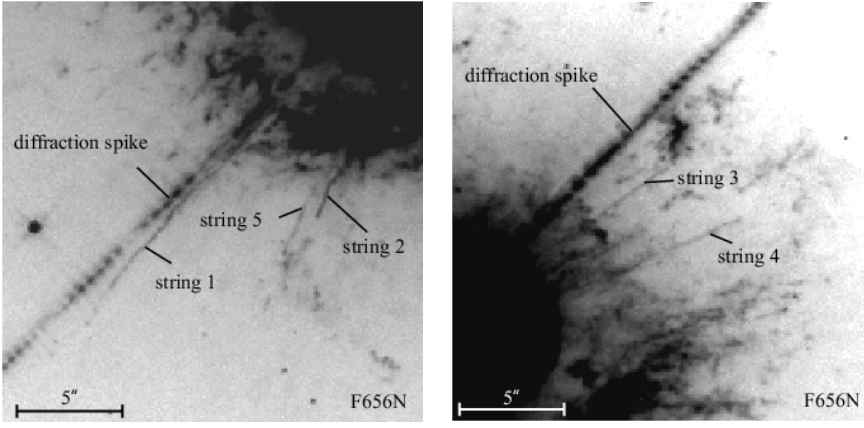


Figure 5: *Left:* Enlargement of the F656N HST image showing the strings 1, 2 and 5 in detail. These three strings are situated to the south-east of  $\eta$  Carinae emerging from the S ridge. *Right:* To the north-east of  $\eta$  Carinae, the strings 3 and 4 are visible.

String 1 is bending slightly, and shows no clear ‘head-like’ structure but a split within the string of about a length of  $1''.5$  near the inner (closer to  $\eta$  Car) part. The other strings are shorter with the smallest in length being string 2 with only  $4''$  (Table 2). On the other hand string 2 is the one with the highest surface brightness and the only one with a sudden change in its (projected) orientation having a kink of about  $22^\circ$ . Strings 3 and 4 are very similar to each other in size and appearance, they are  $7''.6$  and  $9''.3$  long, respectively, and are extremely straight with nearly no variations in surface brightness. String 5 is the faintest, with its surface brightness varying the most.

From the long-slit echelle observations we can derive kinematic information for 3 of the 5 identified strings, namely strings 1, 2 and 5, i.e., the strings south-east of  $\eta$  Carinae (Fig. 5 left). Analyzing these spectra an amazing kinematic behavior was discovered. First of all, the strings are moving with relatively high velocities, the lowest radial velocity measure for string 1 is  $-522 \text{ km s}^{-1}$  at its innermost end (closest to  $\eta$  Car). From there on, outwards along the string, its radial velocity increases steadily up to  $-995 \text{ km s}^{-1}$  at its farthest end. The increase of radial velocity follows a perfectly linear relation, as illustrated in Fig. 6. All strings obey this relationship, they only start with different velocities. If the radial velocities are extrapolated back towards the position of the central star the strings would reach zero radial velocity there within the errors (see position-velocity diagram in Fig. 6). The kinematics of all strings can be described with a kind of Hubble-type law. The velocity gradient of each string is slightly different (see Fig. 6) and amounts to  $2790 \text{ km s}^{-1} \text{ pc}^{-1}$  for string 1,  $3420 \text{ km s}^{-1} \text{ pc}^{-1}$  for string 2 and  $2590 \text{ km s}^{-1} \text{ pc}^{-1}$  for string 5. For none of the other strings kinematic information were available then. Nevertheless due to the overall symmetry of the outer ejecta, it was expected

Table 2: Properties of the strings

string	observed length [pc]	observed width [ $10^{-3}$ pc]	length/width ratio	$v_{\min}$ [ $\text{km s}^{-1}$ ]	$v_{\max}$ [ $\text{km s}^{-1}$ ]
1	0.177	3.0	70	-522	-995
2	0.044	2.0	31	-442	-591
3	0.095	2.0	42	-	-
4	0.103	2.0	68	-	-
5	0.058	2.0	38	-383	-565

that string 3 and 4 are redshifted. A first inspection of our recent HST-STIS observations of the strings (HST-program GO: 8155, PI: Weis) prove that this is the case, adding a further piece of evidence that the strings are also distributed bipolarly.

The  $[\text{N II}]\lambda 6583\text{\AA}/\text{H}\alpha$  ratio for all strings is  $3 \pm 0.3$  and thus comparable to the ratio found in other structures in the nebula around  $\eta$  Carinae.

The physical nature of the strings is not well understood yet. They may or may not be single physical entities. One may think of a coherent structure, similar to a water jet, for instance. However, one may equally well envisage a train of many individual knots or bullets following the same path. One also cannot rule out the possibility that they are trails or wakes following an object at the strings' far ends, or even projection effects of the walls of, for instance, much wider funnels. While their high collimation is most likely due to the fact that the strings move with highly supersonic velocities, it is harder to explain why they follow a Hubble type velocity law. In stellar explosions—rather than winds—a linear velocity profile is a good approximation for the larger radii, close to the head of the explosion (Tscharnutter & Winkler 1979). One may also think—if the time scale of the strings' creation is short compared to the time scale of their evolution since then—that the strings and their expansion velocities can form if this ejection happened with a certain distribution of velocities. Then the fastest part of the string would be the furthest away from the star, leaving the string as a stratified flow or collection of bullet with different velocities. If this would be the case we needed to explain this distribution of initial velocities and answer the question why they did all leave in the same direction? The creation mechanism and physics of the strings is not solved yet and it will be of major interest to now analyze our new HST-STIS data to determine densities and to differentiate between the strings being a flow, a chain of bullets, a knot leaving a trail or something completely different we have not even thought of yet.

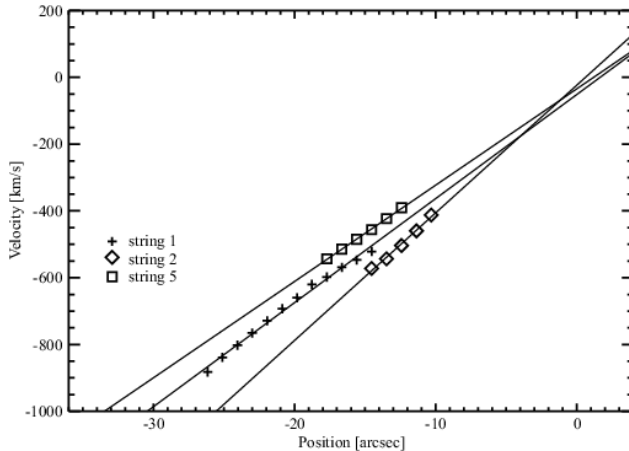


Figure 6: This position-velocity diagram illustrates the constant linear increase of the radial velocity of the strings 1, 2 and 5. Within the errors the radial velocity reaches zero if extrapolated back to the position of the central star.

### 3 The LBV Nebula around HR Car

While located on the sky closely to  $\eta$  Carinae the star HR Carinae is about twice the distance from us at  $5 \pm 1$  kpc (distance measured by reddening; van Genderen et al. 1991). Its spectral type varies from B2 I to B9 I. Strong Balmer, Fe II and [Fe II] emission lines are observed, with the Balmer and Fe II lines showing P Cygni profiles (Carlson & Henize 1979; Hutsemékers & Van Drom 1991), i.e., a more or less classical spectral behavior for an LBV star. HR Car has a luminosity of  $M_{\text{bol}} = -9^{\text{m}}0 \pm 0^{\text{m}}5$ , i.e., at the lower end of the LBV range. A circumstellar nebula around HR Car was discovered only in 1991, making it one of the newest member of the LBV nebulae school (Hutsemékers & Van Drom 1991). The origin and shape of the nebula around HR Car has been discussed by Hutsemékers (1994). A high-resolution image and a spectropolarimetric study have been presented by Clampin et al. (1995). Based on NTT-archive data Fig. 7 shows an image of the nebula around HR Car taken with an  $H_{\alpha}$  filter. The central part in this image is occulted with a chronographic mask, to avoid the saturation of the bright central star.

The nebula around HR Car was originally classified as a filamentary nebula by Nota et al. (1995), showing no clear signs of symmetry. Nevertheless a careful inspection of the image in Fig. 7 leads to the suspicion that the arc in the south-east manifests the brighter part of a lobe structure—as do very faint filaments in the north-west. The underlying nebula may be fainter and reveal a certain symmetry, while the brightest regions do not. To decide on the structure of the nebula around HR Car we obtained high-resolution echelle spectra similar to the way we did for  $\eta$  Carinae. The detailed description

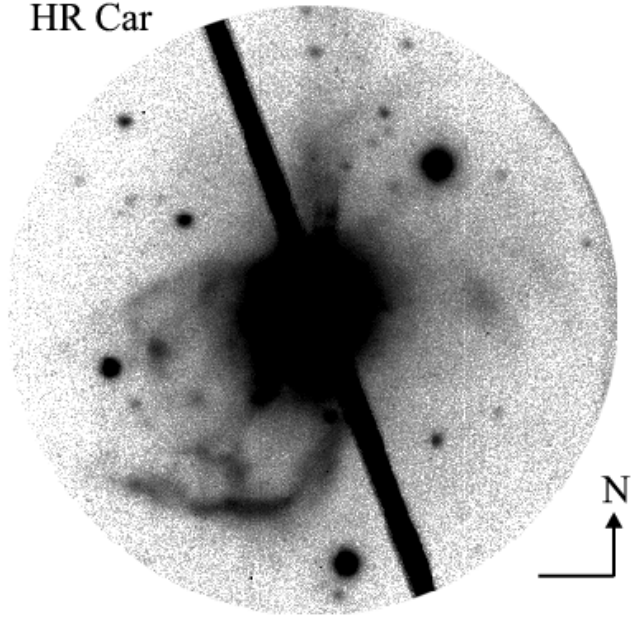


Figure 7: This figure shows an NTT-archive image of the nebula around HR Car with the prominent arc in the south-east, which manifests a brighter structure of the south-eastern lobe.

and analysis can be found in Weis et al. (1997a), here we only summarize the results. Two long-slit spectra crossing the suspected lobes in their center (PA=30°) offset by 13'' north and south of the central star were taken. In both spectra a Doppler ellipse was detected indicating an expansion of  $75 - 150 \text{ km s}^{-1}$ . At both positions a lobe can now be confirmed, with a diameter of 0.63 pc for the north-western one and 0.67 pc for the south-eastern one. The center of expansion of the Doppler ellipse of the lobes differ slightly, the north-western lobe is more redshifted, the south-eastern lobe is blueshifted most likely due to a tilt of the lobes. It was therefore proposed by Weis et al. (1997a) that HR Car exhibits a structure morphologically quite similar to the Homunculus nebula around  $\eta$  Car. Missing is the equatorial disk, but note at this location, a very bright unresolved central part of the nebula around HR Car from where no kinematic data are available yet. This part of the nebula might very well hide a disk or at least its remnants.

If we further compare the nebulae around HR Car and  $\eta$  Car, it seems reasonable to propose that the nebula around HR Car is an older, evolved version of the nebula around  $\eta$  Car. Each lobe in the HR Car nebula is by a factor of 6 larger than those of  $\eta$  Car, and the expansion velocity is by about the same factor lower for HR Car. The LBV nebulae around HR Car and  $\eta$  Car provide therefore an opportunity to probe the evolution of LBV nebulae. In such a scenario (Weis et al. 1997a) the formation of an LBV nebula starts

with a nebula that looks more like the Homunculus (about 150 yrs old) and then evolves into a structure similar to that of HR Car (4000 – 9000 yrs old).

## 4 Bipolar LBV Nebulae—a General Feature?

Are  $\eta$  Carinae and HR Carinae the only bipolar nebulae among LBVs? No—Figure 8 shows a collection of nebulae around LBVs and LBV candidates. Looking at the individual images and determining the nebulae’s morphology it is obvious that none of the nebulae is really spherical. All of them show either an elongation or deviation from spherical symmetry, additional extensions attached to their central body or even a clearly bipolar structure. If we take R 127, an LBV in the LMC and WRA 751 a galactic LBV we find another similar pair. While their central body seems spherical both nebulae show almost triangular extensions which we will call *Caps* in the following. For both nebulae it has been shown (Weis 2000a, b) that these Caps are not only morphological deformations but that they also deviate from the expansion pattern of a sphere. In each case the Cap at one side approaches us, while the other Cap is receding from us. With respect to the central star they represent bipolar components. Analyses of the nebula around AG Car are manifold (Smith 1991, Nota et al. 1992) but still no clear 3D structure could be found. The image nevertheless indicates that the nebula shows at least a deformation in its center, forming a ‘waist-like’ structure. In addition it seems that a second shell is seen in projection underneath or in front of the first shell. For HD 168625 no good kinematic analyses have been published so far—but from the images a two-shell structure seems likely (also mentioned by Nota et al. 1996), probably comparable to the two-shell model for AG Car. In Table 1 the LBV nebulae known today are listed, as well as their sizes and expansion velocities. For all the nebulae sizes the diameter is given or—if asymmetric—at least the diameters along their largest axes. Sizes and velocities separated by a slash indicate that the nebula consists of an inner and an outer shell and both values are given.

I added two LBV candidates to the sample in Fig. 8 as well as to Table 1, the stars Sher 25 in the galactic H II region NGC 3603 and Sk–69° 279 in the LMC. Both stars have not yet been confirmed to be LBVs but their parameters indicate that they are LBVs indeed. For Sher 25 the bipolar structure is already visible from the ground-based image shown here, but its bipolar nature is even more supported by kinematic analyses (Brandner et al. 1997a, Brandner et al. 1997b). Due to the stellar parameters, a possible variability and, a for LBVs quite large nebula with an enhanced  $[\text{N II}]\lambda 6583\text{\AA}/\text{H}\alpha$  ratio, Sher 25 could be an older LBV (bigger size, smaller expansion velocity) like HR Car, putting it towards the end of the evolutionary sequence for LBV nebulae.

The nebula around Sk–69° 279 was first reported by Weis et al. (1995). If Sk–69° 279 is an LBV, the nebulae around it would be the largest LBV nebula known (4.5 pc) with the slowest expansion velocity of  $\approx 14 \text{ km s}^{-1}$ . The

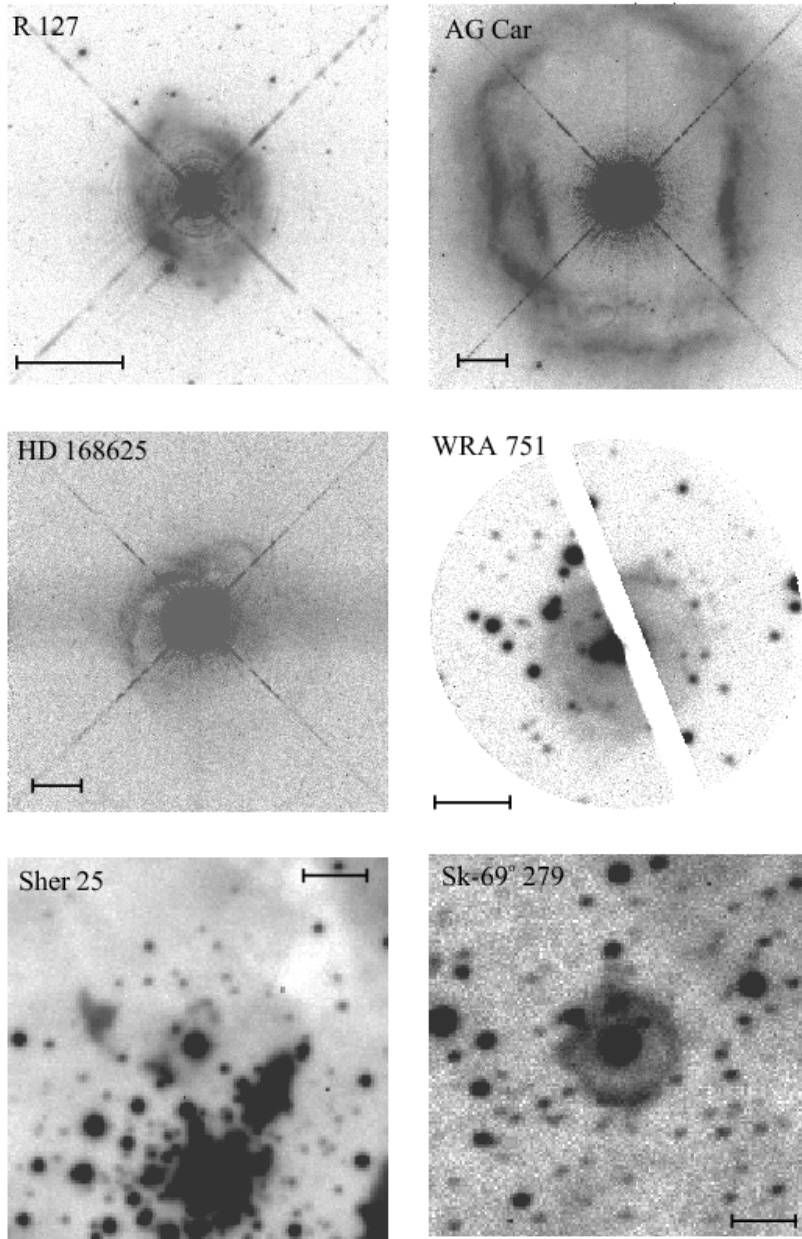


Figure 8: These images show nebula around LBVs and LBV candidates, which indicate an asymmetric—often bipolar—morphology. The scaling bar in each image is  $10''$  in size.

highly enhanced  $[\text{N II}]\lambda 6583\text{\AA}/\text{H}\alpha$  ratio and the star's position in the HRD make Sk-69° 279 another good LBV candidate. This is supported by recent analysis of the stars UV spectrum by Smith Neubig & Bruhweiler (1999). They note that the star is characterized by parameters similar to that of other LBVs. In addition van Genderen (2000) lists the star as an ex/dormant S Dor variable, based on analysis of the star's variability. Its nebula again shows deviations from spherical symmetry especially to the east and a very extended filament stretching to the north, which at first look is easily mistaken as part of the background H II region. Only the kinematic data of this object (Weis et al. 1997b, Weis & Duschl 2000) indicate that this filament is part of the nebula and represents an outflow of gas. We demonstrated that the LBV S 119 also shows such an outflow (Weis et al. 2000a). If outflows in LBV nebulae are common, this will have important implications for the determination of kinematic ages of the nebulae and (determined with help of this method) the true duration of the LBV phase.

The analysis of the nebulae around  $\eta$  Car, HR Car, R 127 and WRA 751 underlines that bipolarity is present in LBV nebulae as a quite common feature. It is by far not unique to  $\eta$  Carinae, as formerly thought.

## 5 Conclusions, Summery and Outlook

Only recently we begin to understand the evolution of massive stars in more detail and especially the consequences for the stars' evolution that result from stellar winds and mass loss. The most massive stars encounter the strongest mass loss and therefore their evolution is affected the most by the wind. This influence of strong mass loss onto the stars' evolution and structure becomes obvious looking at stars more massive than about  $50 M_{\odot}$ . These stars encounter a phase in which they become unstable, variable and loose even more mass in the LBV phase. This phase also marks a sudden change in the evolution of the most massive stars, from redward back to blueward motion in the HRD. LBV nebulae formed in this phase are the relics and doubtless proofs of the stars' high mass loss. Studies of various LBV nebulae have been described here—showing the difference between as well as strong similarities among these nebulae. On the one hand it is obvious that the nebula around  $\eta$  Carinae is special. The extremely filamentary outer ejecta, with its very high expansion velocities of up to  $2000 \text{ km s}^{-1}$  is by no doubts outstanding. It has been proven with kinematic data that beside the bipolar inner Homunculus also the outer ejecta is a highly symmetric bipolar nebula. On the other hand this is not as unique among LBV nebulae as other parameters like the expansion velocities. An LBV nebula which very much looks like the nebula around  $\eta$  Carinae is that around HR Carinae. The bigger size and smaller expansion velocities of the nebula around HR Car support the idea that HR Car is an older, slowed down version of an LBV nebula otherwise similar to that around  $\eta$  Car, which had time to expand for at least 4000 – 9000 years and therefore is bigger.

Quite amazing are the strings in  $\eta$  Carinae: Highly collimated, long and very straight structures expanding with high Mach numbers. Not only is it hard to explain how the strings have been accelerated to such high velocities, they are also following strictly a linear velocity increase along the string, they obey a Hubble-type relation. What creates such a structure, is it a flow, a chain of bullets, a jet, a single knot leaving a trail . . . ? A better understanding of these strange objects may be right on the way with the analysis of our HST-STIS data.

Looking at the morphology and kinematics of other LBV nebula in our Galaxy as well as other neighboring galaxies we found that bipolarity in LBV nebulae is indeed a general feature. Different sizes and expansion velocities of the nebulae can be accounted for by the different ages of the nebulae. Differences in their appearance and expansion may easily be due to interactions with their environments. In that case the known LBV nebulae can be described along an evolutionary sequence. In such a sequence the HR Car nebula, for instance, is an evolved version of  $\eta$  Car's.

Bipolarity in LBV nebulae is a common feature. This poses a new input to the models for stellar evolution and especially the models for the formation of LBV nebulae. Future theoretical work has to incorporate the constraints of bipolarity and find mechanism to conceive this bipolarity. What causes this bipolarity is not known yet. Whether stellar rotation, asymmetrical/bipolar winds or a binary nature could do the job is not clear yet. To decide on that further models for the evolution of LBV stars are desperately needed.

## Acknowledgements

The author is very grateful to Prof. Wolfgang J. Duschl for thoroughly reading and improving the manuscript. Sincere thanks go to Dr. Dominik J. Bomans for several stimulating discussions and helpful comments on the subject. This work was supported by the DFG through grant Du 168/8-1.

## References

- Brandner W., Grebel E.K., Chu Y.-H., Weis K., 1997a, ApJ 475, L45
- Brandner W., Chu Y.-H., Eisenhauer F., Grebel E.K., Points S.D., 1997b, ApJ 489, L153
- Carlson E.D., Henize K.G., 1979, Vistas in Astron. 23, 213
- Chiosi C., Maeder A., 1986, ARA&A 24, 329
- Clampin M., Schulte-Ladbeck R.E., Nota A. et al., 1995, AJ 110, 251
- Currie D.G., Dowling D.M., Shaya E.J., et al. 1996, AJ 112, 1115
- Currie D.G., Dowling D.M., 1999, in *Eta Carinae at the Millennium*, ASP Conf. Ser. 179, eds.: Morse J.A., Humphreys R.M., Damineli A., p. 72
- Damineli A., 1996, ApJ 460, L49
- Damineli A., Conti P.S., Lopes D.F., 1997, New Astronomy 2, 107

- Davidson K., Humphreys R.M., 1997, ARA&A 35, 1
- de Jager C., Nieuwenhuijzen H., van der Hucht K.A., 1988, A&AS 72, 259
- Duschl W.J., Hofmann K.-H., Rigaut F., Weigelt G., 1995, RevMexAA SdC 2, 17
- Figer D.F., Morris M., Geballe T.R., Rich R.M., Serabyn E., McLean I.S., Puetter R.C., Yahil A., 1999, ApJ 525, 759
- García-Segura G., Mac Low M.-M., Langer N., 1996, A&A 305, 229
- Gaviola E., 1946, Revista Astronomica 18, 25
- Gaviola E., 1950, ApJ 111, 408
- Gratton L., 1963, in *Star Evolution*, eds.: Gratton L., New York Academic Press, p. 297
- Humphreys R.M., 1999, in Proc. IAU Collq. No. 169, *Variable and Non-spherical Stellar Winds in Luminous Hot Stars*, eds.: Wolf B., Stahl O., Fullerton A.W., Lecture Notes in Physics, Springer, p. 243
- Humphreys R.M., Davidson K., 1979, ApJ 232, 409
- Humphreys R.M., Davidson K., 1994, PASP 106, 1025
- Humphreys R.M., Davidson K., Smith N., 1999, PASP, 111, 1124
- Hutsemékers D., 1994, A&A 281, L81
- Hutsemékers D., Van Drom E., 1991, A&A 248, 141
- Kudritzki R.P., 1999, in Proc. IAU Collq. No. 169, *Variable and Non-spherical Stellar Winds in Luminous Hot Stars*, eds.: Wolf B., Stahl O., Fullerton A.W., Lecture Notes in Physics, Springer, p. 405
- Kudritzki R.P., Lennon D.J., Haser S.M., Puls J., Pauldrach A.W.A., Venn K., Voels S.A., 1996, in *Science with the Hubble Space Telescope II*, eds.: Benvenuti P. et al., p. 285
- Langer N., Hamann W.-R., Lennon M., Najarro F., Pauldrach A.W.A., Puls J., 1994, A&A 290, 819
- Maeder A., Conti P.S., 1994, ARA&A 32, 227
- Maeder A., Meynet G., 2000, A&A 361, 159
- Massey P., Johnson J., 1993, AJ 105, 980
- Meaburn J., Wolstencroft R.D., Walsh J.R., 1987, A&A 181, 333
- Meaburn J., Walsh J.R., Wolstencroft R.D., 1993a, A&A 268, 283
- Meaburn J., Gehring G., Walsh J.R. et al. 1993b, A&A 276, L21
- Meaburn J., L'opez J.A., Barlow M.J., Drew J.E., 1996a, MNRAS 283, L69
- Meaburn J., Boumis P., Walsh J.R. et al., 1996b, MNRAS 282, 1313
- Morse J.A., Davidson K., Bally J., et al., 1998, AJ 116, 2443
- Nota A., Leithere C., Clampin M., Greenfield P., Golimowski D.A., 1992, ApJ 398, 621
- Nota A., Livio M., Clampin M., Schulte-Ladbeck R., 1995, ApJ 448, 788
- Nota A., Pasquali A., Clampin M., Pollacco D., Scuderi S., Livio M., 1996, ApJ 473, 946

Nota A., Smith L.J., Pasquali A., Clampin M., Stroud M., 1997, ApJ 486, 338  
 Ringuelet A.E., 1958, Zeitschrift für Astrophysik, Bd. 46, p.276  
 Schaerer D., de Koter A., Schmutz W., Maeder A., 1996a, A&A 310, 837  
 Schaerer D., de Koter A., Schmutz W., Maeder A., 1996b, A&A 312, 475  
 Schaller G., Schaerer D., Meynet G., Maeder A., 1992, A&AS 96, 269  
 Smith L.J., 1991 in IAU Symp. 143, *Wolf-Rayet Stars and Interrelations with Other Massive Stars in Galaxies*, eds.: van der Hucht K.A., Hidayat B., Kluwer, Dordrecht, Holland, p. 385  
 Smith L.J., Crowther P.A., Prinja R.K., A&A 281, 833  
 Smith N., Gehrz R.D., 1998, AJ 116, 823  
 Smith Neubig M.M., Bruhweiler F.C., 1999, AJ 117, 2856  
 Stahl O., Damineli A., 1998, in *Cyclical Variability in stellar winds*, proceedings of the ESO workshop, eds.: Kaper L., Fullerton A.W., Springer, p. 112  
 Thackeray A.D., 1949, Observatory 69, 31  
 Thackeray A.D., 1950, MNRAS 110, 524  
 Thackeray A.D., 1961, Obs. 81, 99  
 Tscharnuter W.M., Winkler K.-H., 1979, Comp.Phys.Comm. 18, 171  
 van den Bos, 1938, Union Observatory Circular, No. 100, p.522  
 van Genderen A.M., 2000, A&AS, in press  
 van Genderen A.M., Robijn F.H.A., van Esch B.P.M., Lamers H.J.G.L.M., 1991, A&A 246, 407  
 Viotti R., 1995, RevMexAA SdC 2, 10  
 Walborn N.R., 1976, ApJ 204, L17  
 Walborn N.R., Evans I.N., Fitzpatrick E.L., Phillips M.M., 1991, in IAU Symp. 143, *Wolf-Rayet Stars and Interrelations with Other Massive Stars in Galaxies*, Hrsg.: van der Hucht K.A., Hidayat B., Kluwer, Dordrecht, Holland, p. 505  
 Walborn N.R., 1995, RevMexAA SdC 2, 51  
 Walborn N.R., Blanco B.M., Thackeray A.D., 1978, ApJ 219, 498  
 Walborn N.R., Blanco B.M., 1988, PASP 100, 797  
 Weis K., 2000a, A&A 357, 938  
 Weis K., 2000b, A&A submitted  
 Weis K., Bomans D.J., Chu Y.-H., Joner M.D., Smith R.C., 1995, RevMexAA (SC) 3, 237  
 Weis K., Duschl W.J., Bomans D.J., Chu Y.-H., Joner M.D., 1997a, A&A 320, 568  
 Weis K., Chu Y.-H., Duschl W.J., Bomans D.J., 1997b, A&A 325, 1157  
 Weis K., Duschl W.J., Chu Y.-H., 1999, A&A 349, 467  
 Weis K., Duschl W.J., 2000, A&A submitted  
 Weis K., Duschl W.J., Bomans D.J., 2000a, A&A submitted

